

Control Design for an Under-Actuated UAV Model

M. C. De Simone

Adjunct Professor
University of Salerno
Department of Industrial Engineering
Italy

D. Guida

Full Professor
University of Salerno,
Department of Industrial Engineering
Italy

Unmanned Aerial Vehicles (UAV), are increasingly being adapted and used in civil contexts, with particular specialization in the monitoring of the territory for environmental purposes, civil protection or possibly control and inspection of inaccessible areas or dangerous sites. This concerns, in particular, the adaptation of mini-UAVs, small devices that, due to their manageability and costs, can be allocated for public services. For this reason, it was decided to develop a multibody model of a quadrotor copter in the presence of wind fields by using SimScape Multibody Environment. The quadrotor is modelled as a non-linear under-actuated and strongly coupled system. For the dynamic analysis, aerodynamic effect of drag, the thrust due to the propellers and external wind fields are considered. The evaluation of the needed thrust for prescribed trajectories gives indications about the type of propellers and actuator characteristics to be installed on the UAV.

Keywords: UAV, Feedforward Control, Feedback Control, SimScape, Multibody.

1. INTRODUCTION

Since the early years of their development, Unmanned Aerial Vehicles (UAV) technology has been used for military purposes, from large models to those of the latest generation that have sophisticated and miniaturized sensors, allowing control of the aircraft remotely, so as to complete the mission, without losing lives. Currently, UAVs are used by military forces, by government agencies and from businesses. In the United States, government agencies use some AVs, like the RQ-9 Reaper, to patrol the borders of the nation, with characteristics of exploring and identifying the fugitives. UAVs used for war purposes can be equipped with armaments and/or shooting sensors that allow the sending of the data in real time (both at night and during the day) to control stations, located at kilometres away. Both UAVs and manned aircrafts have similar architecture; the only differences concern the cockpit support systems and the environmental and life control system. Some UAVs carry cameras that weigh much less than a normal adult human being. Despite their heavy loads, armed military drones are lighter than their crew counterpart and same armaments. Small civil UAVs do not have critical systems for survival and are therefore built with lighter but less robust materials, and can use less robust and sophisticated electronic systems. Moreover, the reduced dimensions imply a less sophisticated technology and much less powerful engines, which are not permissible in the normal aircraft equipped with crew. Both the UAVs and the crewed

counterparts may have advanced software for the autopilot, even if the characteristics of this operation may vary. Developing a good architecture a model serves to evaluate the whole functionality, reducing ambiguity and increasing the tangibility of the system. The onboard controller is a low-level system and does not differ much from that used by manned aircraft in order to transmit and receive digital signals a data link is always necessary in order to allow telecommunications between the UAV and the control station. Communication is governed by a protocol that establishes the transmission rules. Unmanned vehicles (such as space vehicles or UAVs) are implemented full or half duplex systems to send control signals and receive telemetry signals. An onboard computer (generally with GPS navigation) connected to the aircraft control system may be used. Flight control and operating system control include the control station (one or more), communication links, data terminals, launch and recovery systems, equipment, ground support and air traffic control interface. UAVs can be programmed to perform aggressive manoeuvres, land, or stayperched on inclined surfaces to observe. An example are the Vertical Take-Off and Landing (VTOL) aircrafts. In order to achieve autonomous control of the aircraft, it is necessary to structure multiple levels of loop control, such as hierarchical control systems. A basic autopilot system includes trim sensors and an onboard processor. Because of the high non-linearity of the plane's dynamics, they are necessary many advanced techniques, including PID control, optimal control methods [1-2], neural networks [3], fuzzy logic [4], and other in order to ensure the desired trajectory [5]. Low-level loops (which control flight) can occur 100 times per second and higher-level loops can be requested with lengths around a second. The basic principle is to break down the behavior of the aircraft into easily manageable

Received: March 2018, Accepted: May 2018
Correspondence to: Dr Marco Claudio De Simone
Department of Industrial Engineering,
Via Giovanni Paolo II, 84135 Fisciano(SA), Italy
E-mail: mdesimone@unisa.it

Doi:10.5937/fmet1804443D

© Faculty of Mechanical Engineering, Belgrade. All rights reserved

FME Transactions (2018) 46, 443-452 **443**

blocks (or layers) with connections between them. The hierarchy of such systems is formed by simple scripts (for finite state machines) to behavior trees and hierarchical work plans. Copters are UAVs whose lift is generated by four or more independent rotors. Hardware selection and integration is usually based on heuristics. Building a realistic copter simulator requires accurate modeling and knowledge of its dynamics and the effect of each component on that. Often, moving from simulation to actual experiment is a challenging task due to the huge dynamical differences when working with the real system [6]. A quadrotor is a high nonlinear system because of the coupling of the aerodynamic forces of the four rotors and an underactuated system due to the fact that the 6 degrees of freedom are controlled by only four actuators. Furthermore, due to their small size and weight, this class of aircraft is very susceptible towards nonlinearities like atmospheric turbulence and reacts especially sensitive to system degradation [7]. Nonlinear control approaches like nonlinear inverse dynamics (NID) allow for counteracting these problems under the condition of well-known model parameters. Because system identification for this class of aircraft often is not valid throughout the complete flight envelope, neural networks are used to compensate these model errors [8]. For such reasons, there has been a great development in the area of multi-rotor control, e. g. [9–15], where the quadrotor dynamics is approximated with a linear system and a standard linear controller is designed [16-19]. Ryll et al.(2016) investigate a new type of UAV concept which is able to smoothly change its configuration from underactuated to fully actuated by using only one additional motor that tilts all propellers at the same time. FAST-Hex can adapt to the task at hand by finely tuning its configuration from the efficient (but underactuated) flight (typical of coplanar multi-rotor platforms) to the full-pose-tracking (but less efficient) flight, which is attainable by non-coplanar multi-rotors [20]. Falconi and Melchiorri (2012) propose, starting from a well-known quadrotor model, to introduce features in order to create an over-actuated quadrotor able to fly performing manoeuvres that are typically not feasible for UAVs. The goal has been reached by using inverse dynamics control scheme in order to control the modified flying vehicle, with particular attention to the asset control [21]. Antonio-Toledo et al. (2016) present a twin control strategy of the quadrotor based on inner (attitude control) and outer (position control) loops. The outer loop generates the inputs for inverse dynamics and calculates instantaneous desired angles for inner loop to stabilize the orientation of the vehicle. In addition, a recurrent high order neural network and extended Kalman filter are used to identify motors dynamics [22]. Askari et al.(2015) underline a second aspect related to formation control strategies when a large number of unmanned aerial vehicles are involved. The authors base their control laws for formation control both on classical theory and inverse dynamics, and then present a comparison study [23]. Zang et al. (2016) address the topic of cooperative trajectory planning problem mathematically formulated as a decentralized receding horizon optimal control

problem (DRH-OCP). Furthermore, the authors investigate on a decentralized coordination strategy for multi-vehicle real-time trajectory planning designed by effectively combining the benefits of inverse dynamics optimization method and receding horizon optimal control technique [24]. Trajectory control and formation control strategies are particularly important in the case of UAVs for agricultural applications and in case of surveying and measurement activities [25-28].

In creating a dynamic model of a UAV, the main difficulties are represented by the parametrization and modelization of external disturbances, such as wind gusts, that deteriorate the quadrotor abilities and, cause instabilities [29-31]. On the other hand, Stevanović and Rašuo (2017) show how, by using the basic principles of bionics, with the help of modern software engineering, it is possible to conduct dynamical analysis of new mechanisms inspired by insects, in 3D environment obtaining excellent and complete results [32]. In this study, we present a quadcopter multi-body model developed in SimScape Multi-body Environment, that allows to build very detailed models by using 3D Cad geometries [33-40]. For controlling such model, an inverse dynamic analysis and a standard PID controller have been developed [41-46]. Such study anticipates a subsequent experimental analysis to be conducted in X-Plane aircraft simulator. Inverse dynamics control. The main scope of inverse dynamics analysis and feed-forward control law is to construct an inner loop control based on the motion base dynamic model which, in the ideal case, exactly linearizes the nonlinear system and an outer loop control to drive tracking errors to zero. The PID linear controller is considered in the second part of the paper, where the effect of wind fields will be taken into account.

One novel aspect that is considered in this article is represented by the study of the aerodynamics of the propellers that, in general, affects the dynamic response and performance of the UAVs. It depends on the different flight conditions because it is important to include relative wind velocity and gusts [47-48].

The paper is organized as follows. Section 2 discusses the quadrotor mathematical model. In section 3, particular attention is given to the treatment of the thrust forces generated by each propeller while section 4 contains the numerical simulations and some details about the prescribed trajectory given to the quadrotor. It is divided into two parts: the first part relates to the inverse dynamic analysis of the model, while the second part is dedicated to the feedback control law evaluation in presence of wind disturbances. The final section presents the conclusions.

2. MATHEMATICAL MODEL

The geometry was obtained by using a Cad file geometry of a quadcopter assembled in SolidWorks environment. In Figure 1, the copter is reported with axes reference system and propeller labelling, mounted at the end of each cross arm. The rotors are driven by DC electric motors powered by electronic speed controllers. In all the flight configurations, one pair of opposite propellers rotate clockwise, while the other

pair rotates anticlockwise: in this way it is possible to avoid the yaw drift due to reactive torques and the lateral motion without changing the pitch of the propeller blades. Fixed pitch simplifies rotor mechanics and reduces the gyroscopic effects. Control is obtained by imposing different speeds to different propellers, so they will produce differential aerodynamic forces and moments. To ensure the hovering condition, all four propellers need to rotate at the same speed; the vertical motion is possible because the speed of all four propellers is increased or decreased by the same amount, simultaneously.

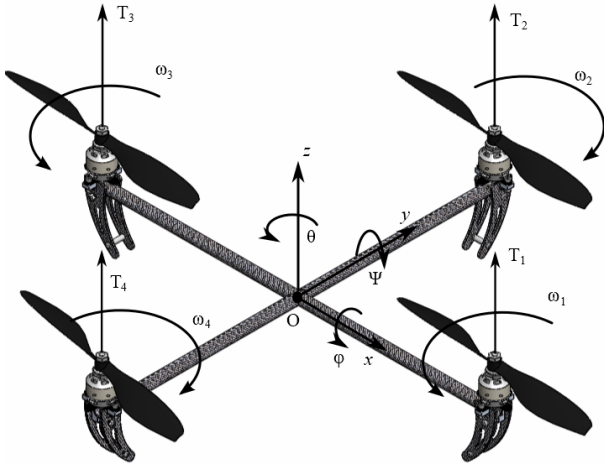


Figure 1. Quadrotor configuration of the body axis system

From Figure 1, therefore we can deduce that if we want to change the pitching angle, the speed of propeller 1 and 3 must be changed conversely. In this way, the pitching rotation and the lateral movement in the x -direction are allowed. Similarly, for roll and corresponding lateral motion along the y -axis, the speed of propellers 2 and 4 must be changed conversely. To produce yaw motion around the z -axis, the speed of one pair of two oppositely placed propellers must be increased while the speed of the other pair must be decreased by the same amount. In this way, the total thrust produced by all the propellers is the same, but differential drag moment creates yawing motion. Let I denote a right-hand inertial frame and B the right-hand body fixed frame whose origin coincides with the centre of mass of the vehicle. By using the notation of the Euler angles, it is possible to obtain the rotation matrix from I to B , i.e.

$$R_{\{I-B\}} = \begin{bmatrix} R_{11} & R_{12} & R_{13} \\ R_{21} & R_{22} & R_{23} \\ R_{31} & R_{32} & R_{33} \end{bmatrix} \quad (1)$$

where:

$$\begin{aligned} R_{11} &= c(\theta)c(\psi) \\ R_{12} &= -s(\theta) \\ R_{13} &= c(\theta)s(\psi) \\ R_{21} &= c(\varphi)c(\psi)s(\theta) + s(\varphi)s(\psi) \\ R_{22} &= c(\theta)c(\varphi) \\ R_{23} &= c(\varphi)s(\psi)s(\theta) - c(\varphi)c(\psi) \\ R_{31} &= c(\psi)s(\varphi)s(\theta) - c(\varphi)s(\psi) \\ R_{32} &= c(\theta)s(\varphi) \\ R_{33} &= c(\varphi)c(\psi) + s(\varphi)s(\psi)s(\theta) \end{aligned}$$

where c and s are shorthand forms for cosine and sine respectively. The dynamic model is derived in the hypothesis that the structure is rigid and the propellers are rigid in plane. In (2) the translational equations of motion of the drone in the coordinate system I is reported:

$$M\dot{v} = - \begin{bmatrix} 0 \\ 0 \\ mg \end{bmatrix} + R_{\{I-B\}} \begin{bmatrix} 0 \\ 0 \\ T \end{bmatrix} - F \quad (2)$$

where $v = [\dot{x} \ \dot{y} \ \dot{z}]^T$ is the absolute velocity vector of the center of gravity of the vehicle in the inertial frame, M represents the mass matrix, g is the gravitational acceleration, m is the total mass of the system, T is the total upward thrust, and vector F represents the principal non-conservative forces applied to the quadrotor airframe by the aerodynamics of the rotors. In particular, F has two contributions, drag force acting because of the relative motion of the quadrotor and wind disturbances. The rotational acceleration of the body frame is given by Euler's equation of motion gives:

$$J\dot{\omega} = -\omega \times \omega J + \Gamma \quad (3)$$

where $J \in \mathbf{R}^{3 \times 3}$ denotes the constant inertia matrix of the system (expressed in the body-fixed frame B), ω is the angular velocity vector and $\Gamma = [\tau_x \ \tau_y \ \tau_z]^T$ is the torque due to aerodynamic forces applied to the frame.

3. TWO DIMENSIONAL DYNAMIC MODEL

For this analysis, we considered a simplified 2D model. For such model, rolling, yawing and translation along the y -axis equations are considered satisfied, so the equations of motion of the reduced system are reported in (4).

$$\begin{cases} -m\ddot{x} + T_x - F_{D_x} + F_{W_x} = 0 \\ -m\ddot{z} - mg + T_z - F_{D_z} + F_{W_z} = 0 \end{cases} \quad (4)$$

In (5), the condition constraint for the pitch angle is reported, since the value cannot be set arbitrary.

$$\frac{T_x}{T_z} = \tan(\psi) \approx \psi \quad (5)$$

where T_x and T_z are respectively the two components of the total thrust along the x and z -direction. Regarding the pitching torque system of equations reported in (3), such relations becomes a scalar equation with pitching torque τ_y different from zero.

4. AERODYNAMIC FORCES AND TORQUES

The thrust force T_i produced from each propeller is proportional to the square of its angular speed rotation using momentum theory [49] as reported in (6).

$$T_i = b\omega_i^2, \quad i = 1, 2, 3, 4 \quad (6)$$

The main error of this model is represented by the simplistic assumption underlying (6) that the thrust

forces are directly proportional to the square of the motor speed. In reality, they are complex functions of the motor speed and environmental conditions. Regarding the drag force, (7) describes such term, that is proportional to the translational velocity of drone [50].

$$F_D = \frac{1}{2} \rho S C_D V^2 \quad (7)$$

where S is the cross-sectional area of the quadrotor and $C_D = \text{diag}(C_{Dx}, C_{Dy}, C_{Dz})$ is the translational drag coefficient matrix.

4.1 Aerodynamics of vertical and Forward flight

A rotor generates thrust by inducing a velocity on the air that passes through it. In hovering (quadrotor maintains a constant position over the ground), the thrust generated from each propeller is directly linked to v_h , vertical induced velocity on the air without relative velocity between the rotor and the air. Such relations is derived from the momentum analysis and reported in (8).

$$v_h = \sqrt{\frac{T_{i,h}}{2\rho A}} \quad (8)$$

The relative velocity between the rotor plane and the surrounding air V and the pitching angle ψ , also, influences the thrust produced by each rotor. Furthermore, from the blade element theory, the thrust expression becomes:

$$T_i = c_t \rho \pi R_p^4 \omega_i^2 \quad (9)$$

In (9), the air density is indicated with ρ and the radius of the propeller is reported with R_p . When $\psi = 0$ rad, the quadrotor is in vertical climb or descent flight and the thrust coefficients c_t can be evaluated by (10).

$$c_t = \frac{nca}{4\pi R_p} \left(\beta_t - \frac{v_h \pm V}{\omega R_p} \right) \quad (10)$$

with n is the number of blades on each propeller, c is the blade chord, a is the lift slope curve and β_t is the pitch angle at the blade tip that is function of rotor geometry alone as we are considering fixed pitch rotors [51].

Equation 10 is derived in the hypothesis of constant chord and linear twist and assuming uniform inflow. So, finally, it is possible to find the angular velocities ω_i which produce the thrust for a given vertical velocity $V = \dot{z}$ and given geometric parameters. In forward flight, $V = \dot{x}$, it is important to consider the angle of attack of the model, so the equation for the thrust coefficient becomes:

$$c_t = \frac{nca}{4\pi R_p} \left(\frac{\beta_t}{3} + \frac{V^2 \beta \cos^2 \psi}{2\omega_i^2 R_p^2} + \frac{V \sin \psi + v_h}{2\omega R_p} \right) \quad (11)$$

In this work, we decided to investigate in more detail the influence of the c_t parameter on the evaluation of the thrust force for every flight conditions, instead of using a constant value as generally done. In order to test the reliability of (10) and (11), the results are compared with an experimental database [52].

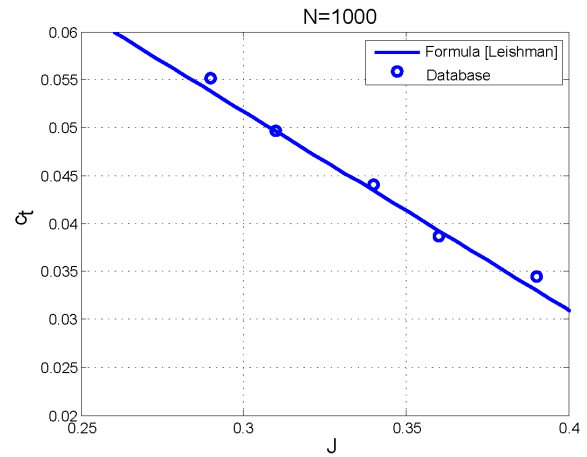


Figure 2. Thrust coefficients comparison

In the graph, the comparison between the values of the thrust coefficients obtained from the database reported by using blue circles and the curve obtained from (10) is reported [53]. In Figure 2, the thrust coefficients are plotted against J , whose expression is reported in (12).

$$J = \frac{V}{ND_p}$$

where N is the angular velocity in rpm and D_p represents the diameter of the propellers.

5. NUMERICAL SIMULATIONS

For the numerical simulation, we include rotor dynamics and external perturbations such as wind disturbances. By using a geometry obtained by means of a CAD software, we can create a much more detailed model in which the distribution of the masses can reproduce in simulation a much more truthful behaviour. For this reason, we developed a multibody model in SimScape Multi-body environment [54]. Mass matrix and inertia matrix are obtained by using a CAD model of the quadcopter prototype and are represented by the following expressions (12, 13), i.e.

$$M = \begin{bmatrix} 0.37958 & 0 & 0 \\ 0 & 0.37958 & 0 \\ 0 & 0 & 0.37958 \end{bmatrix} \text{kg} \quad (12)$$

$$I = \begin{bmatrix} -0.0053 & -2.492e^{-0.5} & 1.249e^{-0.5} \\ -2.492e^{-0.5} & 0.0092 & 7.245e^{-0.5} \\ 1.249e^{-0.5} & 7.245e^{-0.5} & 0.0043 \end{bmatrix} \text{kgm}^2 \quad (13)$$

The equivalent mathematical model used for the evaluation of the control laws is reported in (14), i.e.

$$\begin{cases} T = M\dot{v} + F(v) \\ \tau_y = I_{yy}\ddot{\psi} + M_D(\dot{\psi}) \end{cases} \quad (14)$$

where $T = \sum_{i=1}^4 T_i$ and $\tau_y = d(T_1 - T_3)$. In the general case, F contains the gravity effects, the aerodynamic

drag terms and the wind disturbances contributions, while M_D is function of the aerodynamic drag moment. The respective boundary conditions for every segment of the trajectory are reported in table 1, while velocity and acceleration boundary conditions are all set equal to zero. By solving (14), it is possible to derive the laws of motion for the three degrees of freedom (x -axis, z -axis and pitch angle ψ) and the feed-forward controllaws of the four propeller T_1 , T_2 , T_3 and T_4 necessary to obtain the desired trajectory. From the thrust forces, the standard procedure is to evaluate the angular velocities that each motor must deliver in order to ensure the tracing of the desired trajectory by using (6).

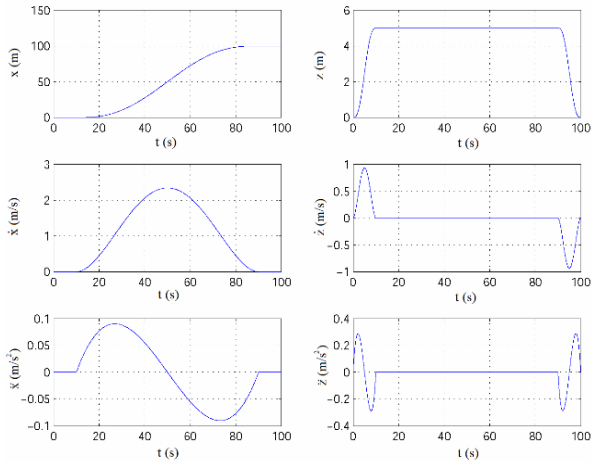


Figure 3. Law of motion for x -axis and z -axis

Evaluated the angular velocities in the traditional way and ascertained that, as shown in Figure 2, expressions (10) and (11) approximate the experimental values correctly, we extrapolated c_b , that it is function not only of N , but also of the relative velocity V . In Figure 4 we have reported for each time integration the extrapolated values of b against the constant values used previously. In this way, it is possible to have the corrected angular velocities for every time step.

5.1 Inverse Dynamics Analysis in the absence of wind disturbances

Given the translational equations of motion of the 2DOF model of UAV, forces are evaluated through an inverse dynamics analysis.

Table 1. Waypoint coordinates used for the desired trajectory

	x [m]	Y [m]	Z [m]	T_{fin} [s]
WP_1	0	0	0	0
WP_2	0	0	5	10
WP_3	100	0	5	90
WP_4	100	0	0	100

At this stage, the effect of wind disturbances is not considered. By solving (14) in SimScape environment, it is possible to evaluate the forces that must be applied to the model in order to follow the predetermined trajectory. In Figure 3, are depicted the laws of motion for x -axis, z -axis evaluated for the desired trajectory.

The angular velocities of each propeller are calculated from the thrust forces. We have compared the

values obtained by using a constant thrust coefficient and an interpolated coefficient value and they are plotted respectively in Figure 5 and Figure 6.

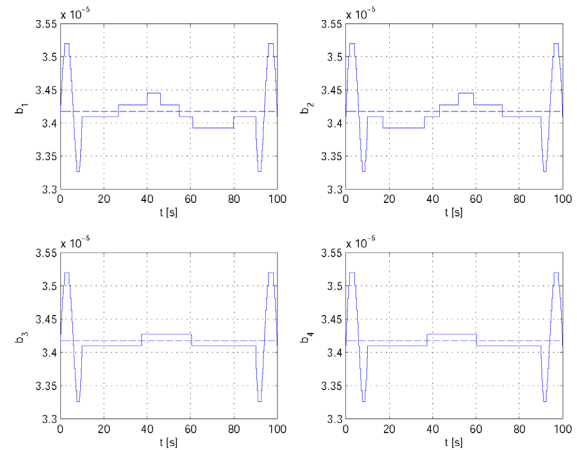


Figure 4. Comparison between constant b coefficient and interpolated b coefficient

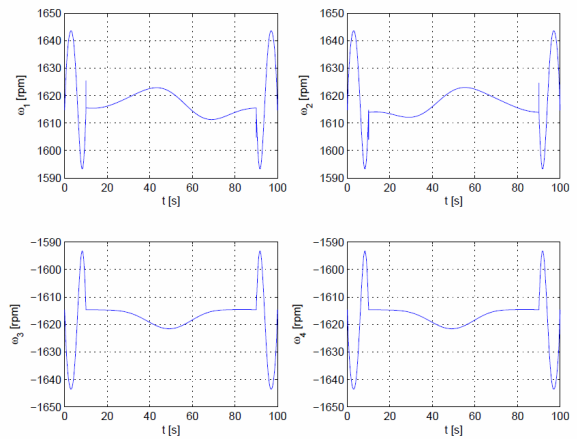


Figure 5. Feed-forward angular velocity of each propeller by using constant thrust coefficient

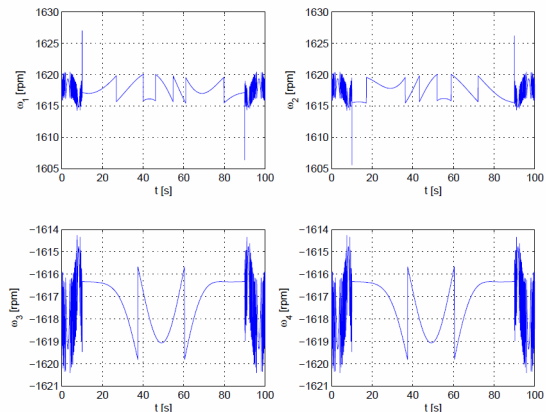


Figure 6. Feed-forward angular velocity of each propeller by using interpolated thrust coefficient

5.2 Forward Dynamics Analysis in Presence of wind disturbances

In this section, two different feedback controllers are considered in order to take into account the aerodynamic disturbances represented by wind gusts. The first controller is designed in order to evaluate the necessary thrust force to follow the target trajectory

while the second controller ensures the necessary pitch angle. To counteract these effects, PID controllers are developed and reported in eq. 15 and 16, i.e.

$$F_{fb,Thrust}(t) = K_p e(t) + K_d \dot{e}(t) + K_i \int_0^t e(t) dt \quad (15)$$

And

$$M_{fb,\psi}(t) = K_p e_\psi(t) + K_d \dot{e}_\psi(t) + K_i \int_0^t e_\psi(t) dt \quad (16)$$

where K_p , K_d and K_i respectively represent the proportional, derivative and integral gain values vector. The error signal vectors have the following expression

$$e(t) = \begin{bmatrix} e_x(t) \\ 0 \\ e_z(t) \end{bmatrix} = \begin{bmatrix} x_{ref}(t) - x(t) \\ 0 \\ z_{ref}(t) - z(t) \end{bmatrix} \quad (17)$$

$$e_\psi(t) = \psi_{rif}(t) - \psi(t) = \tan^{-1} \left(\frac{T_{x,FB}}{T_{z,FB}} \right) - \psi(t) \quad (18)$$

where $[x_{ref} \ 0 \ z_{ref}]^T$ is the desired trajectory, and $e_\psi(t)$ is the pitching error signal. As suggested by Chen et al. (2013), the wind field is modelled as an external force term, so that, in the balance equations (14), F is the sum of three contributions [50], i.e.

$$F(\dot{v}) = F_D(\dot{v}) - mg + F_W(v) \quad (19)$$

To test the robustness of the controller, the vehicle is subjected to two wind fields $W_1 = [2 \ 0 \ 0]^T$ m/s and $W_1 = [2 \ 0 \ 1.5]^T$ m/s. The two control thrust laws have been traced back, through the use of (6), to the values of the angular velocities required by the four engines and they have been reported respectively in Figure 5 for constant thrust coefficient and in Figure 6 for interpolated thrust coefficients. The first oscillations that characterize each curve of the angular velocity relative to W_1 for the first timestep are due to the sudden arrangement that the system must have in order to adapt to the presence of the wind field.

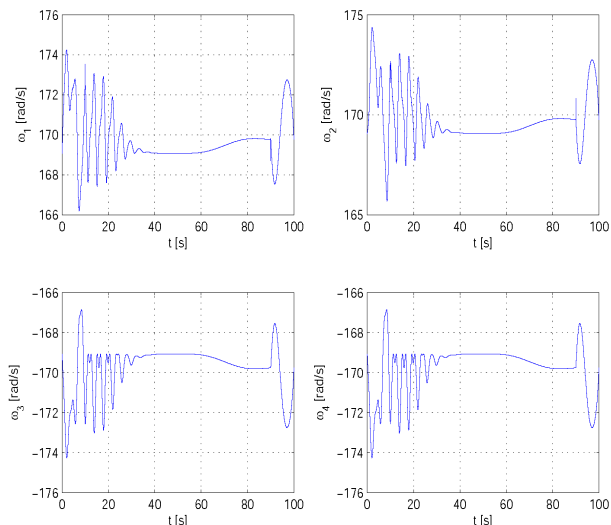


Figure 7. Closed Loop Angular Velocities of the Propellers with Constant Thrust Coefficient Subjected to W_1 Wind Field

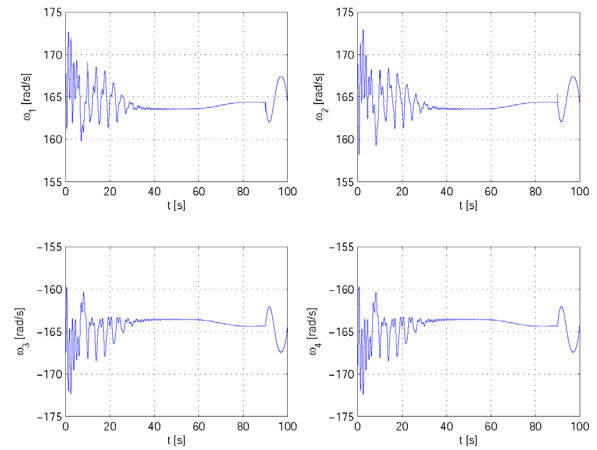


Figure 8. Closed Loop Angular Velocities of the Propellers with Constant Thrust Coefficient Subjected to W_2 Wind Field

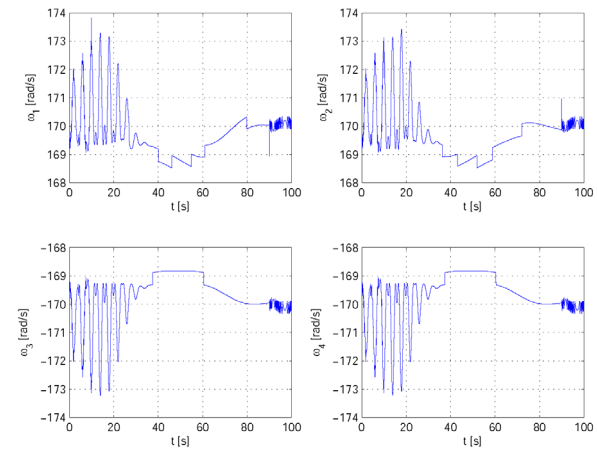


Figure 9. Closed Loop Angular Velocities of the Propellers with Interpolated Thrust Coefficient Subjected to W_1 Wind Fields

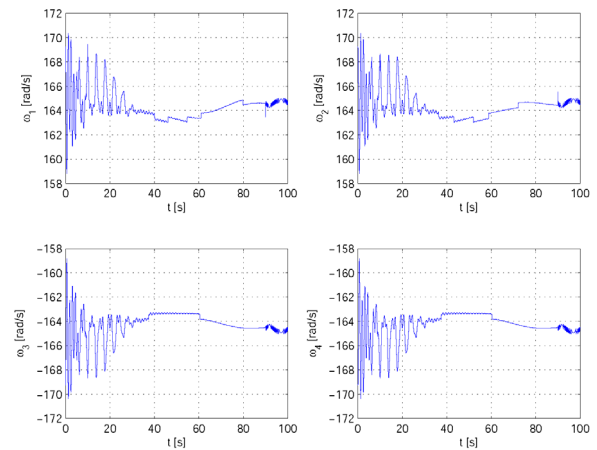


Figure 10. Closed Loop Angular Velocities of the Propellers with Interpolated Thrust Coefficient Subjected to W_2 Wind Fields

6. CONCLUSIONS

The ever-increasing use of UAVs in different sectors ranging from surveillance to precision agriculture requires increasingly effective control techniques. For this reason, the need arises to create increasingly accurate models on which to design control laws. To

achieve this, the SimScape multibody and multi-physics modelling environment allows the integration of CAD software with Matlab calculation software, enabling the use of more accurate mass distribution models. In this paper, despite the usual approach followed in practice to consider the thrust coefficient b to be constant, we also investigated the use of values of such coefficient updated based on the flight parameters of the UAV. The author's research is focused on multi-body dynamics [55-58], finite element methods [59-63], system identification [64-66], optimal control [67-76] and vibrations in presence of friction [77-81]. This work represents for the authors the starting point for a more extensive experimental activity in which a new UAV class will be designed and simulated through the use of open-source software such as ROS-Gazebo and using certified simulators like X-Plane. In the first part of the paper, in order to evaluate the open loop control laws, an inverse dynamics analysis is performed on the UAV model for feed forward thrust evaluation for a given trajectory. For the evaluation of such control thrust, only the aerodynamic effect of drag is considered and the pitching angle motion law is evaluated together with the pitching torque required. Thereafter, considering also the action of wind gusts a feedback control was designed by using two linear PID controllers. The comparison between the real and the desired paths have demonstrated the effectiveness of the projected closed-loop control. For both cases of open-loop and closed-loop thrust laws, we have verified the reliability of the hypothesis of a constant thrust coefficient that is generally made in these applications. Since it is generally the function of the engine rpm, of the thrust forces required and of the relative velocity of the vehicle and its variation with these parameters is not negligible, all the values are extrapolated from different curves parameterized as a function of the rpm for every timesteps. Comparison of the results shows that by using a constant coefficient instead of an interpolated value, there is an error in estimating the correct rpm of about ± 30 rpm.

REFERENCES

[1] Sharifzadeh, M., Farnam, A., Senatore, A., Timpone, F. and Akbari, A. Delay-dependent criteria for robust dynamic stability control of articulated vehicles, *Mechanisms and Machine Science*, 2018, 49, pp. 424-432

[2] Sharifzadeh, M., Timpone, F., Senatore, A., Farnam, A., Akbari, A. and Russo, M. Real time tyre forces estimation for advanced vehicle control, *International Journal of Mechanics and Control*, 2017, 18 (2), pp. 77-84.

[3] De Simone M. C., et al.: Ultrasonic Sensors for Object Recognition by Using Neural Network Algorithms for ROS applications, *Robotics*, 2018, accepted for publication.

[4] Nemes, A. Mester, G. Unconstrained evolutionary and gradient descent-based tuning of fuzzy-partitions for UAV dynamic modeling (2017) *FME Transactions*, 45 (1), pp. 1-8, doi: 10.5937/fmet1701001N

[5] Stojkovic, I. and Katic, D. Formation control of robotized aerial vehicles based on consensus-based algorithms (2017) *FME Transactions*, 45 (4), pp. 559-564, doi: 10.5937/fmet1704559S

[6] Shaqura, M. and Shamma, J.S. An Automated Quadcopter CAD based Design and Modeling Platform using Solidworks API and Smart Dynamic Assembly, *ICINCO 2017 - Proceedings of the 14th International Conference on Informatics in Control, Automation and Robotics*, 2, pp. 122-131, 2017.

[7] Mirkov, N., Rasuo, B.: Maneuverability of an UAV with COANDA effect based lift production (2012) *28th Congress of the International Council of the Aeronautical Sciences 2012, ICAS 2012*, 3, pp. 1745-1750.

[8] Schnetter, P., Marcinek, M., Krueger, T., Voersmann, P. Adaptive Flight Control Using Second Order Sliding Mode Online Learning. In *AIAA Infotech@ Aerospace (I@A) Conference* (p. 5133), 2013.

[9] Mirkov, N., Rašuo, B. Numerical simulation of air jet attachment to Convex walls and application to UAV (2015) *Lecture Notes in Computational Science and Engineering*, 108, pp. 197-207, doi: 10.1007/978-3-319-25727-3_15

[10] Belkheiri, M., Rabhi, A., Hajjaji, A. E., Pegard, C. Different linearization control techniques for a quadrotor system, 2nd ed. *Int. Conf. on Communications, Computing and Control Applications (CCCA)*, 1-6, 2012.

[11] Tomazic, T. and Drago, M. Model based UAV autopilot tuning, *Proceedings of the 8th WSEAS international conference on fluid mechanics*, 8th WSEAS international conference on Heat and mass transfer. *World Scientific and Engineering Academy and Society (WSEAS)*, 2011.

[12] Chelaru, Teodor-Viorel, Valentina, and Adrian Chelaru. "Dynamics and flight control of the Huang, UAV formations." *WSEAS Transactions on Systems and Control* 4.4 (2009): 198-210.

[13] Chelaru, Teodor-Viorel, and Valentin Pana. "Stability and control of the UAV formations flight." *WSEAS Transactions on systems and Control* 5.1 (2010): 26-36.

[14] Yaou, Z. H. A. N. G., et al. The Attitude Control of the Four Rotor Unmanned Helicopter Based on Feedback Linearization Control, *WSEAS Transactions on Systems* 4.

[15] B. Zhu, W. Huo, Trajectory linearization control for a quadrotor helicopter, *8th IEEE Int. Conf. on Control and Automation (ICCA)*, pp. 34-39, 2010.

[16] S. L. W. Gabriel, M. Hoffmann and C. J. Tomlin, Quadrotor helicopter trajectory tracking control, *Proc. of the AIAA Guidance Navigation and Control Conference*, 2008.

[17] S. Bouabdallah, A. Noth and R. Siegwart, PID vs LQ control techniques applied to an indoor micro quadrotor, *Proceedings of the IEEE/RSJ International Conference on Intelligent Robots and Systems* 3, pp. 2451 - 2456, 2004.

- [18] Salazar-Cruz, S., Palomino, A. and Lozano, R. Trajectory tracking for a four rotor mini-aircraft, 44th IEEE Conference on Decision and Control and European Control Conference CDCECC' 05, 2005, pp. 2505–2510.
- [19] Salih, A. L., Moghavvemi, M., Mohamed, H. A. F. and Gaeid, K. S. Modelling and PID controller design for a quadrotor unmanned air vehicle, Proceeding of IEEE International Conference on Automation, Quality and Testing Robotics (AQTR), 2010, pp. 1 - 5.
- [20] Ryll, M., Bicego, D. and Franchi, A. (2016, October). Modeling and control of FAST-Hex: a fully-actuated by synchronized-tilting hexarotor. In Intelligent Robots and Systems (IROS), 2016 IEEE/RSJ International Conference on (pp. 1689-1694). IEEE.
- [21] Falconi, R. and Melchiorri, C. Dynamic model and control of an over-actuated quadrotor uav. IFAC Proceedings Volumes, 45(22), 192-197, 2012.
- [22] Antonio-Toledo, M. E., Sanchez, E. N. and Alanis, A. Y. Robust neural decentralized control for a quadrotor UAV. In Neural Networks (IJCNN), 2016 International Joint Conference on (pp. 714-719). IEEE.
- [23] Askari, A., Mortazavi, M. and Talebi, H. A. UAV formation control via the virtual structure approach. Journal of Aerospace Engineering, 28(1), 04014047, 2013.
- [24] Zhang, Y., Yang, J., Chen, S. and Chen, J. (2015, December). Decentralized cooperative trajectory planning for multiple UAVs in dynamic and uncertain environments. In Intelligent Computing and Information Systems (ICICIS), 2015 IEEE Seventh International Conference on (pp. 377-382). IEEE.
- [25] Chen, S., McDermid, G. J., Castilla, G. and Linke, J. Measuring Vegetation Height in Linear Disturbances in the Boreal Forest with UAV Photogrammetry. Remote Sensing, 9(12), 1257, 2017.
- [26] Langhammer, J., Bernsteinová, J. and Miřijovský, J. Building a High-Precision 2D Hydrodynamic Flood Model Using UAV Photogrammetry and Sensor Network Monitoring. Water, 9(11), 861, 2017.
- [27] Adão, T., Hruška, J., Pádua, L., Bessa, J., Peres, E., Morais, R. and Sousa, J. J. Hyperspectral imaging: A review on UAV-based sensors, data processing and applications for agriculture and forestry. Remote Sensing, 9(11), 1110, 2017.
- [28] Ortega-Terol, D., Hernandez-Lopez, D., Ballesteros, R., Gonzalez-Aguilera, D. Automatic Hotspot and Sun Glint Detection in UAV Multispectral Images. Sensors, 17(10), 2352, 2017.
- [29] Alexis, K., Nikolakopoulos G. and Tzes, A. Switching model predictive attitude control for a quadrotor helicopter subject to atmospheric disturbances, Control Engineering Practice 19, 2011, pp. 1195-1207
- [30] Powers, C., Mellinger, D., Kushleyev, A., Kothmann, B., Kumar, V. Influence of Aerodynamics and proximity effects in quadrotor flight, Proceedings of the 13th International Symposium on Experimental Robotics, Quebec city, Canada, June 17-21, 2012.
- [31] Mirkov, N., Rašuo, B. Numerical simulation of air jet attachment to convex walls and applications (2010) 27th Congress of the International Council of the Aeronautical Sciences 2010, ICAS 2010, 2, pp. 1615-1621.
- [32] Stevanović, I., Rašuo, B. Development of a miniature robot based on experience inspired by nature (2017) FME Transactions, 45 (1), pp. 189-197, doi: 10.5937/fmet1701189S
- [33] De Simone, M.C., Russo, S., Rivera, Z.B. and Guida, D.: Multibody Model of a UAV in Presence of Wind Fields, in: Programme and Proceedings of the International Conference on Control, Artificial Intelligence, Robotics and Optimization (ICCAIRO 2017), 20-22.05.2017, Prague, Czech Republic.
- [34] Zhang Y., Li Z., Gao J., Hong J., Villecco F. and Yunlong L.: A method for designing assembly tolerance networks of mechanical assemblies. Mathematical Problems in Engineering Vol. 2012, Article number 513958, 2012.
- [35] Formato A., Ianniello D., Villecco F., Lenza T.L.L. and Guida D.: Design optimization of the plough working surface by computerized mathematical model, Emirates Journal of Food and Agriculture, Vol. 29, No. 1, pp. 36-44, 2017.
- [36] Villecco F. and Pellegrino A.: Entropic measure of epistemic uncertainties in multibody system models by axiomatic design, Entropy, Vol. 19, No. 7, Article number 291, 2017.
- [37] Concilio, A., De Simone, M.C., Rivera, Z.B. and Guida, D.: A New Semi-Active Suspension System for Racing Vehicles, FME Transactions, Vol. 45, No. 4, pp. 565–571, 2017.
- [38] Senatore E., De Simone, M.C., Rivera, Z.B. and Guida D. Integrated Open Source Robotic Framework for Unmanned Airships, Robotics, 2018, accepted for publication
- [39] Villecco, F., Pellegrino, A. Evaluation of uncertainties in the design process of complex mechanical systems (2017) Entropy, 19 (9), art. no. 475, doi: 10.3390/e19090475
- [40] Zhai, Y., Liu, L., Lu, W., Li, Y., Yang, S., Villecco, F. The application of disturbance observer to propulsion control of sub-mini underwater robot (2010) Lecture Notes in Computer Science (including subseries Lecture Notes in Artificial Intelligence and Lecture Notes in Bioinformatics), 6016 LNCS (PART 1), pp. 590-598, doi: 10.1007/978-3-642-12156-2-44
- [41] Iannone, V., et al. Control Law Design for UGVs by Using Inverse Dynamic Analysis, Machines, 2018, accepted for publication
- [42] Quatrano, A., De Simone, M.C., Rivera Z.B. and Guida, D.: Development and Implementation of a

- Control System for a retrofitted CNC Machine by using Arduino. *FME Transactions*, Vol. 45, No. 4 pp. 578–584, 2017.
- [43] Sena, P., Attianese, P., Carbone, F., Pellegrino, A., Pinto, A. and Villecco, F., 2012, “A Fuzzy Model to Interpret Data of Drive Performances from Patients with Sleep Deprivation”, *Computational and mathematical methods in medicine*.
- [44] Pellegrino, A. and Villecco, F., 2010, “Design Optimization of a Natural Gas Substation with Intensification of the Energy Cycle”, *Mathematical Problems in Engineering*, 294102.
- [45] Ghomshei, M., Villecco, F., Porkhial, S. and Pappalardo, M.: Complexity in Energy Policy: a Fuzzy Logic Methodology, in: *Proceeding of Sixth International Conference on, IEEE7 Fuzzy Systems and Knowledge Discovery, FSKD'09.*, pp. 128-131, 2009.
- [46] De Simone, M.C. and Guida, D.: Dry Friction Influence on Structure Dynamics, in: *Proceedings of the 5th ECCOMAS Thematic Conference on Computational Methods in Structural Dynamics and Earthquake Engineering (COMPdyn 2015)*, 25-27.05.2015, Crete Island, Greece, pp.4483–4491.
- [47] Alexis, K., Nikolakopoulos, G. and Tzes, A. Switching model predictive attitude control for a quadrotor helicopter subject to atmospheric disturbances, *Control Engineering Practice* 19,2011, pp. 1195-1207
- [48] Powers, C., Mellinger, D., Kushleyev, A., Kothmann, B. and Kumar, V. Influence of Aerodynamics and proximity effects in quadrotor flight, *Proceedings of the 13th International Symposium on Experimental Robotics*, Quebec city, Canada, June 17-21, 2012.
- [49] Bramwell, A. R. S., Done, G. and Balmford, D. *Bramwells Helicopter Dynamics*, 2nd ed., Butterworth Heinemann, Oxford, UK, 2001.
- [50] Chen, Y., He, Y. and Zhou, M. Modeling and control of a quadrotor helicopter system under impact of wind field, *Research Journal of Applied Sciences, Engineering and Technology* 6(17), 2013, pp. 3214-3221.
- [51] Leishman, J.G. *Principles of Helicopter Aerodynamics*, Cambridge Aerospace Series 2000.
- [52] <http://www.drivencalc.de/>
- [53] De Simone, M.C. and Guida D. Identification and control of a Unmanned Ground Vehicle by using Arduino, *UPB Scientific Bulletin, Series D: Mechanical Engineering*, 80(1), 2018, pp 141-154.
- [54] Pappalardo, C. M., Guida, D. Dynamic Analysis of Planar Rigid Multibody Systems modeled using Natural Absolute Coordinates, *Applied and Computational Mechanics*, 2018, accepted for publication.
- [55] Pappalardo, C. M. and Guida, D. On the Lagrange Multipliers of the Intrinsic Constraint Equations of Rigid Multibody Mechanical Systems, *Archive of Applied Mechanics*, 2018, 88(3), pp. 419-451.
- [56] Pappalardo, C. M. and Guida, D. On the use of Two-dimensional Euler Parameters for the Dynamic Simulation of Planar Rigid Multibody Systems, *Archive of Applied Mechanics*, 2017, 87(10), pp. 1647-1665.
- [57] Pappalardo, C. M. A Natural Absolute Coordinate Formulation for the Kinematic and Dynamic Analysis of Rigid Multibody Systems, *Nonlinear Dynamics*, 2015, 81(4), pp. 1841-1869.
- [58] Villecco, F. On the Evaluation of Errors in the Virtual Design of Mechanical Systems, *Machines*, 2018, accepted for publication.
- [59] Pappalardo, C. M., Zhang, Z., and Shabana, A. A Use of Independent Volume Parameters in the Development of new Large Displacement ANCF Triangular Plate/Shell Elements, *Nonlinear Dynamics*, 2018, 91(4), pp. 2171-2202.
- [60] Pappalardo, C. M., Wang, T. and Shabana, A. A. Development of ANCF Tetrahedral Finite Elements for the Nonlinear Dynamics of Flexible Structures, *Nonlinear Dynamics*, 2017, 89(4), pp. 2905-2932.
- [61] Pappalardo, C. M., Wang, T. and Shabana, A. A. On the Formulation of the Planar ANCF Triangular Finite Elements, *Nonlinear Dynamics*, 2017, 89(2), pp. 1019-1045.
- [62] Pappalardo, C. M. et al. A New ANCF/CRBF Fully Parametrized Plate Finite Element, *ASME Journal of Computational and Nonlinear Dynamics*, 2017, 12(3), 031008, pp. 1-13.
- [63] Pappalardo, C. M., Yu, Z., Zhang, X. and Shabana, A. A. Rational ANCF Thin Plate Finite Element, *ASME Journal of Computational and Nonlinear Dynamics*, 2016, 11(5), 051009, pp. 1-15.
- [64] Pappalardo, C. M. and Guida, D. System Identification and Experimental Modal Analysis of a Frame Structure, *Engineering Letters*, 2018, 26(1), pp. 56-68.
- [65] Guida, D., Nilvetti, F., and Pappalardo, C. M. Parameter Identification of a Two Degrees of Freedom Mechanical System, *International Journal of Mechanics*, 2009, 3(2), pp. 23-30.
- [66] Guida, D., and Pappalardo, C. M. Sommerfeld and Mass Parameter Identification of Lubricated Journal Bearing, *WSEAS Transactions on Applied and Theoretical Mechanics*, 2009, 4(4), pp. 205-214
- [67] Pappalardo, C. M., and Guida, D. Adjoint-based Optimization Procedure for Active Vibration Control of Nonlinear Mechanical Systems, *ASME Journal of Dynamic Systems, Measurement, and Control*, 2017, 139(8), 081010, pp. 1-11.
- [68] Kulkarni, S., Pappalardo, C. M., and Shabana, A. A. Pantograph/Catenary Contact Formulations, *ASME Journal of Vibrations and Acoustics*, 2017, 139(1), 011010, pp. 1-12
- [69] Pappalardo, C. M., Guida, D. Control of Nonlinear Vibrations using the Adjoint Method, *Meccanica*, 2017, 52(11-12), pp. 2503-2526.
- [70] Pappalardo, C. M., Patel, M. D., Tinsley, B. and Shabana, A. A. Contact Force Control in Multibody

Pantograph/Catenary Systems, Proceedings of the Institution of Mechanical Engineers, Part K: Journal of Multibody Dynamics, 2016, 230(4), pp. 307-328.

- [71] Guida, D., and Pappalardo, C. M. Control Design of an Active Suspension System for a Quarter-Car Model with Hysteresis, *Journal of Vibration Engineering and Technologies*, 2015, 3(3), pp. 277-299.
- [72] Guida, D., and Pappalardo, C. M. Forward and Inverse Dynamics of Nonholonomic Mechanical Systems, *Meccanica*, 2014, 49(7), pp. 1547-1559.
- [73] Guida, D., and Pappalardo, C. M. A New Control Algorithm for Active Suspension Systems Featuring Hysteresis, *FME Transactions*, 2013, 41(4), pp. 285-290.
- [74] Ruggiero, A., De Simone, M.C., Russo, D. and Guida, D. Sound pressure measurement of orchestral instruments in the concert hall of a public school, *International Journal of Circuits, Systems and Signal Processing*, 2016, 10, pp. 75-812.
- [75] De Simone, M.C., Rivera, Z.B. and Guida, D. Obstacle Avoidance System For Unmanned Ground Vehicles By Using Ultrasonic Sensors, *Machines*, 2018, accepted for publication
- [76] De Simone, M.C., Guida, D.: On the Development of a Low Cost Device for Retrofitting Tracked Vehicles for Autonomous Navigation, in: *Proceedings of the XXIII Conference of the Italian Association of Theoretical and Applied Mechanics (AIMETA 2017)*, 4-7.09.2017, Salerno, Italy.
- [77] Guida, D., Nilvetti, F., and Pappalardo, C. M. Instability Induced by Dry Friction, *International Journal of Mechanics*, 2009, 3(3), pp. 44-51.
- [78] Guida, D., Nilvetti, F., and Pappalardo, C. M. Dry Friction Influence on Cart Pendulum Dynamics, *International Journal of Mechanics*, 2009, 3(2), pp. 31-38.
- [79] De Simone, M.C. and Guida, D. Modal coupling in presence of dry friction, *Machines*, 2018, 6(1), 8, doi: 10.3390/machines6010008
- [80] De Simone, M.C., Rivera, Z.B., Guida, D. Finite element analysis on squeal-noise in railway applications, *FME Transactions*, 2018, 46(1), pp. 93-100.
- [81] Ruggiero, A., Affatato, S., Merola, M. and De Simone, M. C. FEM analysis of metal on UHMWPE total hip prosthesis during normal walking cycle, in: *Proceedings of the XXIII Conference of the Italian Association of Theoretical and Applied Mechanics (AIMETA 2017)*, 4-7.09.2017, Salerno, Italy.

NOMENCLATURE

$R_{\{I-B\}}$	Rotation matrix
φ	Roll
ψ	Pitch
θ	Yaw
m	Mass
J	Inertia
T	Total thrust
Γ	Torque due to aerodynamic forces
F_D	Drag force vector
C_D	Drag coefficient matrix
P	Air density
S	Cross-sectional area
V	Vertical Velocity
b	Thrust parameter
ω	Angular velocity of the propeller
c_t	Thrust coefficient
R_p	Radius of the propeller
n	Number of blades
c	Blade chord
a	Lift slope curve
β_t	Pitch angle at the blade tip
N	Angular velocity in rpm
D_p	Diameter of the propeller
F_w	Wind field force

ПРОЈЕКТОВАЊЕ УПРАВЉАЊА КОД МОДЕЛА БЕСПИЛОТНЕ ЛЕТЕЛИЦЕ СА МАЊИМ БРОЈЕМ АКТУАТОРА

М.Ц. Де Симоне, Д. Гуида

Беспилотне летелице се све више прилагођавају и користе у цивилне сврхе, нарочито за надгледање подручја у циљу очувања животне средине, цивилне заштите или контролу и испитивање неприступачних терена и опасних места. Ово се нарочито односи на мини беспилотне летелице, мале уређаје који захваљујући својој управљивости и трошковима могу да се користе у јавним службама. Све наведено нас је подстакло да израдимо мултибоди модел квадротора за услове поља ветра применом система SimScape Multibody Environment. Квадротор је моделиран као спрегнути нелинеарни систем са мањим бројем актуатора. Динамичком анализом обухваћен је аеродинамички утицај чеоног отпора, потисак који стварају пропелери и спољашња поља ветра. Евалуација потиска потребног за пројектоване трајекторије показује какав тип пропелера и какве карактеристике треба да има актуатор за уградњу у беспилотну летелицу.